Very High Cycle Fatigue Tests with a Resonance-Regulated Device for Testing of Large-Scale Cast Iron and Steel Specimens

Peter Schaumann[1], Luka Radulovic[1], Jan Kulikowski[1], Attila Alt[2]
[1] Leibniz University Hannover, Institute for Steel Construction - ForWind,
Hannover, Germany
[2] Sole proprietorship,
Meersburg, Germany

ABSTRACT

A new resonance-regulated testing device operating at a frequency of up to 200 Hz has been developed for very high cycle fatigue tests on large-scale cast iron and steel specimens. The device is able to perform tests on axially loaded plate specimens with a thickness of up to 20 mm and a width of up to 40 mm. It allows testing with a maximum amplitude of 70 kN and a stress ratio of $0.1 \leq R \leq 0.5$. In this paper, the working principle of the device is shown. Furthermore, the calibration, pretension and testing procedures are presented based on the tests with ductile cast iron specimens (EN-GJS-18C-LT).

KEY WORDS: fatigue testing device, very high cycle fatigue, butt joints, cast iron

INTRODUCTION

Offshore wind turbines are expected to experience up to 10^9 load cycles during their service life (Seidel, 2010). Thus, the fatigue limit state represents a crucial factor during the design process. In current offshore standards and guidelines (DIN 18088-3, 2019; DNVGL-RP-C203, 2016; DNVGL-ST-0361, 2016), the design S-N curves do not allow for an endurance limit. These S-N Curves are mostly derived from fatigue tests up to 10^7 load cycles. The shape of S-N curves for more than 10^7 load cycles and the question of the existence of an endurance limit are still of particular interest of ongoing research (Schaumann and Steppeler, 2013; Steppeler, 2014). The investigation of this range requires testing facilities able to perform a very high number of cycles (beyond 10^7) within a reasonable timeframe. Over the last decades, different servo-hydraulic, resonant, forced-vibration, rotating-bending and ultrasonic machines for very high cycle fatigue tests have been developed (Stanzl-Tschegg, 2014). The testing frequency of these machines lies between several hundred Hz in case of servo-hydraulic machines to up to 20 kHz for the ultrasonic testing equipment. One of the main limitations of these machines is that only small-sized specimen can be tested. This yields to a smaller testing volume, which reduces the probability of encountering large defects. Hence, higher fatigue strength can be measured (Furuya, 2010). Considering offshore wind turbines with some structural components whose wall thicknesses exceed 100 mm, it is necessary to perform tests on large-scale specimens to limit possible scale effects. An improved experimental basis of fatigue tests is vital for optimization of these structures.

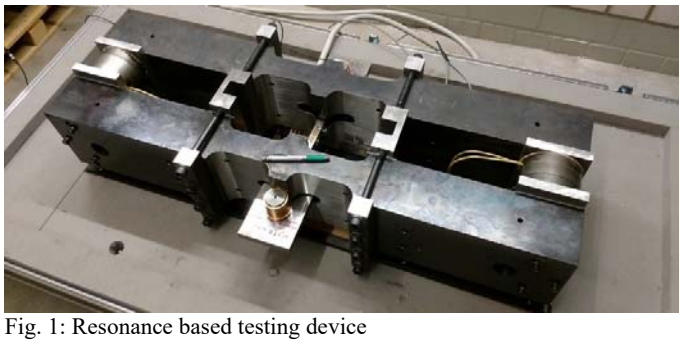

Fig. 1: Resonance based testing device

For this reason a novel resonance-regulated testing device operating at a frequency of up to 200 Hz has been developed (Fig. 1). The device is made for axial fatigue tests on the butt welds and ductile cast iron specimens in the range of 10^7 to $2 \cdot 10^8$ load cycles. The device is not a universal testing machine but it is shaped and designed for a predefined geometry of specimens. Tests on plate specimens with a thickness of up to 20 mm and a width of up to 40 mm are possible. Fatigue tests with a testing device based on the same operating principle (Alt, 2007), limited to specimens with a thickness of 5 mm, had already been carried out on butt welds (Schaumann and Keindorf, 2007; Steppeler, 2014). A comparison between two devices and the improvements implemented in the new resonance-based device can be found in Schaumann et al. (2017).

As a resonance based machine, the operating frequency of the testing device is highly sensitive to modifications of geometry or of material properties of the specimen. The dynamic calibration factor is non-linearly depending on the operating frequency. The implemented control considers linear dependency only. Therefore, the device must be calibrated for each new type of specimen. Furthermore, the mean stress level cannot be readjusted during the test. Thus, the losses of the mean stress occurring during the test are studied and quantified.

The tests results presented in this paper are based on the tests performed with specimens made of ductile cast iron (EN-GJS-18C-LT), commonly used for casting of nacelle components of wind turbines.

OPERATIONAL PRINCIPLE

The operational principle of the resonance-regulated testing device for large-scaled test specimens is based on the German patent DE 10204258 (Alt, 2007) and illustrated in Fig. 2. The device is composed of a resonance frame and a control system. The resonance frame has the shape of a closed rectangular frame consisting of two longitudinal steel beams connected with two crosspieces (Fig. 3). The body consisting of resonance frame and specimen oscillates at the first natural frequency of the body. The nodal points of the first mode are in the corners of the frame (Fig. 2). The specimen is fixed between the longitudinal beams in the center of the frame. Due to the symmetry of the first shape mode, the specimen is subjected to purely axial load. The extended ends of the longitudinal beams are used as lever arms for the application of the load induced via alternating current (AC) magnets.

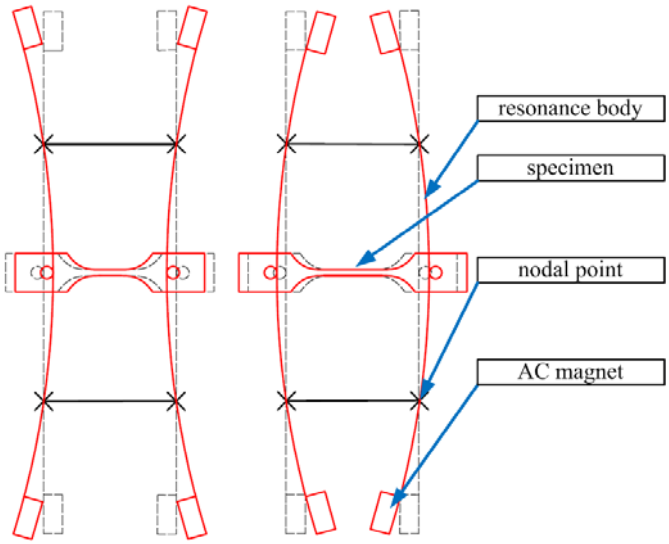

Fig. 2: Operational principle of the testing device

The entire control loop of the testing device consists of a set of strain gauges and an accelerometer applied on the resonance frame, measurement amplifiers, control unit, power amplifier and AC magnets. The strain gauges and the accelerometer are attached at one longitudinal beam of the frame and continuously measure the deformation and acceleration of the beam. These quantities are proportional to the loading of the specimen and they are used for monitoring and adjustment of the loading. The measured signals of deformation and acceleration are amplified and processed by the control unit. The control unit adjusts the measured accelerometer signal with the set point by actuating the AC magnets via the power amplifier. Phase information is used to allow for excitation with natural frequency which allows for stable oscillation during the whole test. The load amplitude of the specimen depends on the power input in the AC magnets. The currently used power amplifier BEAK BPS 1016-P V1, with a maximal output power of 7 kW, allows tests with a load amplitude of up to 70 kN.

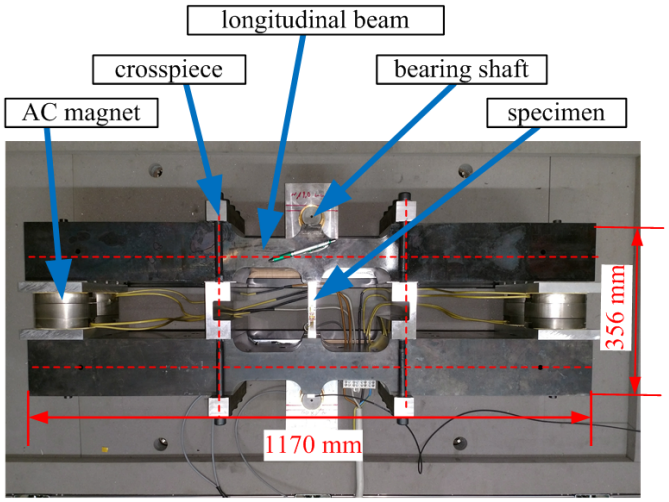

Fig. 3: Components and dimensions of the resonance frame

Bearing and Geometry of the Specimen

The resonance-regulated testing device enables tests on steel and casted iron specimens with a thickness of up to 20 mm. The specimen is installed in the resonance frame through the gap at the center of the longitudinal beams (Fig. 4). These gaps lie in the symmetry plane of the testing device. Two bearing shafts allow the transfer of the load between the frame and the specimen. In order to fit the bearing shafts, the specimen has two holes on its outer sides. The holes have the same diameter as the shafts. The hole tolerance H7 ensures a tight fit. Two rings made of brass, the inner diameter of which corresponds to the diameter of the shaft, are centered below and above the specimen´s hole and the shaft is installed through them. The rings prevent a direct contact of the bearing shaft and the steel beams which would cause wearing of the beams during repeated tests. With this kind of bearing, friction losses are avoided, and only axial load is induced in the specimen.

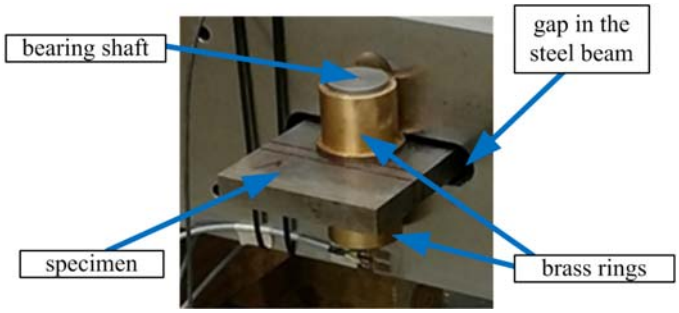

Fig. 4: The bearing of the specimen via bearing shaft

The holes in the specimen cause notch stresses. The specimens have to be designed such that a crack is initiated in the nominal cross section rather than in the holes. This is especially important for smooth cast iron specimens without notch. Considering these limitations, the ductile cast iron specimens can have a maximum width of 20 mm (Fig. 5). Due to higher notch stresses at the welding seem, steel samples can be designed with a width of up to 40 mm.

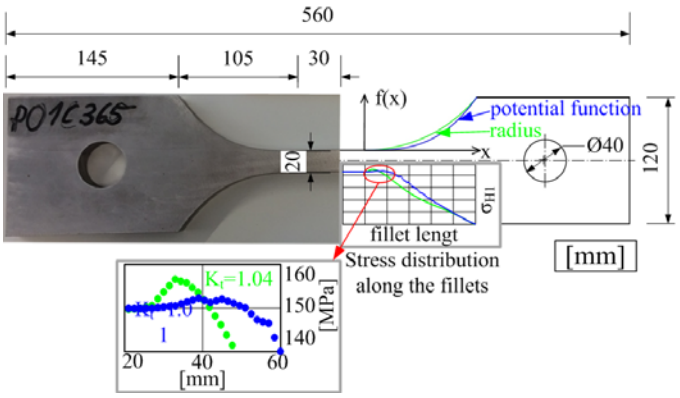

Fig. 5: Ductile cast iron specimen (left); comparison of distribution of first principal stress along the fillets defined via constant radius and via potential function (right) (Schaumann et al., 2017)

The final design of specimens is featured by a rectangular nominal cross section with tangential transitional fillets between the testing region and the load introduction regions on the sample's ends (see Fig. 5) (Schaumann et al., 2017). Recommendations according to ISO 1099 (2006) have been taken into account. The goal is to obtain a stress distribution along the specimen as constant and uniform as possible. The optimization of transitional fillets has been performed based on Zenner and Buschermöhle (1996) and Shirani and Härkegård (2011). Instead of applying a constant radius, a set of potential functions of the type $f(x) = (x/a)^b$ describing the geometry of the fillet has been studied. In this way, the stress concentration in the transition region can be smoothed almost completely. For example, in case of specimens with a thickness of 20 mm, by designing the fillets with potential function $f(x) = (x/28.5)^3$ the stress concentration factor was reduced to $K_t = 1.01$. The comparison of stress distribution along the fillets designed with constant radius (green) and designed with optimized potential function (blue) is shown in Fig. 5 (right).

Pretension

The fixation of the specimen on the steel beams provides form closure only in direction of tensile loading. As shown in Fig. 6, a tensile preload which is greater or equal to the amplitude of the dynamic loading, is required to allow for dynamic loading without gapping.

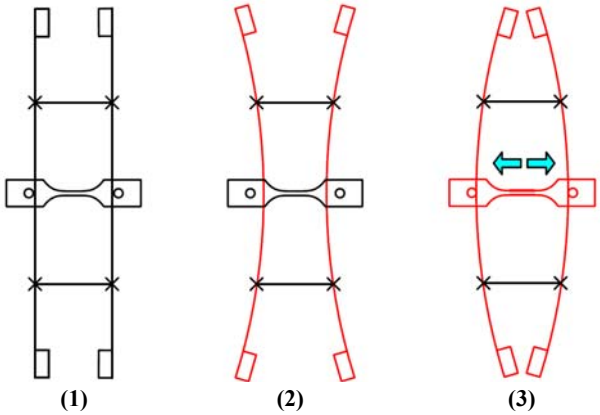

Fig. 6: Frame and specimen deformation during a load cycle without pretension: (1) initial position, (2) minimal distance between the longitudinal beams, (3) maximal distance between the longitudinal beams

Hence, only tests with pulsating tensile loads ($R > 0$) are possible. A fixation of the sample with form closure in both, tensile and compressive direction was avoided because of two reasons. By switching the area of shaft contact within each load cycle, the damping of the natural frequency would have increased significantly. Also buckling of the specimen might have become an issue.

The preload is achieved by increasing the distance between the longitudinal bars after the specimen has been installed in the frame. For this purpose, the bolts which are holding tight the crosspieces are loosened, and a hydraulic cylinder is used to create the necessary gap between the longitudinal beam and the crosspieces. Then, thin steel plates are inserted in this gap. After the steel plates have been set, the hydraulic cylinder is removed, and the bolts of the crosspiece are tightened again (Fig. 7). The thickness of the plates varies between 1.0 mm and 2.0 mm.

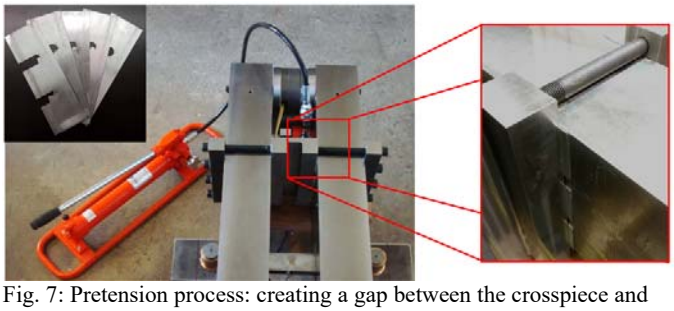

Fig. 7: Pretension process: creating a gap between the crosspiece and the longitudinal beams with a hydraulic cylinder in order to set thin steel plates used for pretension (upper left corner)

Due to the manufacturing tolerances the brass rings are not in contact with the longitudinal beams after the specimen is installed. The pretension plates are used to fill the gap first and then preload the beams versus specimen second. Once the gap is closed, a further increase of plate thickness of 0.04 mm yields to an increase of 10 MPa of tensile stress in the specimen. Different plate thicknesses are required to compensate for length tolerances of the specimen.

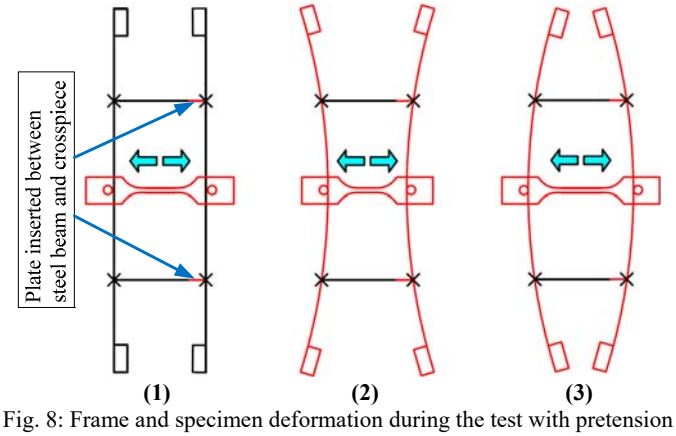

Fig. 8: Frame and specimen deformation during the test with pretension applied: (1) Initial position, (2) minimal distance between the longitudinal beams, (3) maximal distance between the longitudinal. beams

The stress introduced in the specimen via the pretension process represents the mean stress of the subsequent fatigue test. Hence, the specimen remains under tension during the entire load cycle as shown in Fig. 8. The bending deformation of the frame caused by the pretension of the specimen is neglected in Fig. 8 (1) for the sake of simplicity.

CALIBRATION

During a standard test no sensor is applied on the specimen. The level of pretension is measured via a set of strain gauges and the load amplitude via accelerometer both applied on the longitudinal steel beam of the resonance frame. Both signals need calibration to allow for translation of their voltage output into the unit of the applied force. For this purpose some specimens were equipped with strain gauges to be able to act as an axial force sensor by themselves. The strain gauges and accelerometer on the steel beam were calibrated by operating the testing device with the calibration specimens.

In case of fatigue tests on the ductile cast iron specimens with a nominal cross section of 20 mm x 20 mm (see Fig. 5), the calibration specimens have respective nominal widths of 18 mm, 20 mm and 22 mm. The different widths of calibration specimens ensure that the obtained calibration factors are valid for any eventual stiffness variation of the standard specimens used for the fatigue tests. Such stiffness variations are caused by slight variations of geometry and/or material properties between different specimens.

It will be demonstrated below that the dynamic calibration factor for the accelerometer is depending on the natural frequency of the testing device only. Within an extended frequency range this dependency is non-linear. Within the concerned frequency range for the 18 mm to 22 mm specimen a linear approach is fully sufficient. The control loop considers such linear dependency only which makes another calibration necessary if frequency respectively the material or type of specimen changes significantly.

Static Calibration of the Calibration Specimen

Prior to the calibration of the test frame, all calibration specimens are calibrated in a conventional hydraulic test machine. The specimens are axially loaded at different levels of load. A measurement amplifier connected to the strain gauges measures the voltage correspondent to each level of axial strain caused by the applied load. In this way, a relationship between the axial strain in the specimen (measured in volts) and the applied force is established.

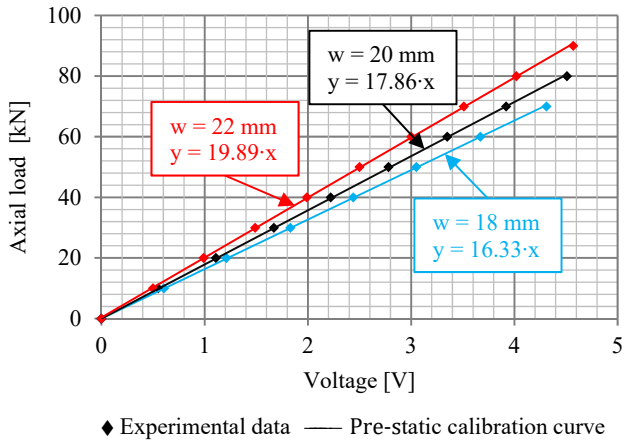

Fig. 9: Pre-calibration of the specimens in a conventional hydraulic test machine (w = width of specimen)

It is a linear relationship described with the linear regression lines of the experimental data. The slope of the line represents the calibration factor (k_{ps}). The calibration samples are then used in the resonance-regulated test device to calibrate its strain gauge and accelerometer signals of preloading and load amplitude, respectively. Prior to the pre-calibration tests, the results of which are shown in Fig. 9, each specimen underwent two preload cycles up to the level of maximal force applied during the calibration to minimize hysteresis effects.

Static Calibration of the Test Device

The static calibration allows to read the preload from the strain gauge signal of the resonance-regulated test device. To determine the static calibration factor, the previously calibrated specimens are installed in the test device and pre-loaded to five different levels. The control unit acquires the measurements of the strain gauges on the longitudinal beam of the frame and provides as the output bending of the beam in digits of a 10 bit AD converter. The strain gauges applied on the longitudinal bars are set in a bridge configuration which measures bar's strain caused by bending. The linear regression of the relationship between the preload applied according to calibration specimen and response of the test device represents the static calibration curve and its slope is the static calibration factor (Fig. 10). The static calibration factor (k_s) has a value of $k_s = 11.96 \cdot 10^{-2}$ for ductile cast iron specimens.

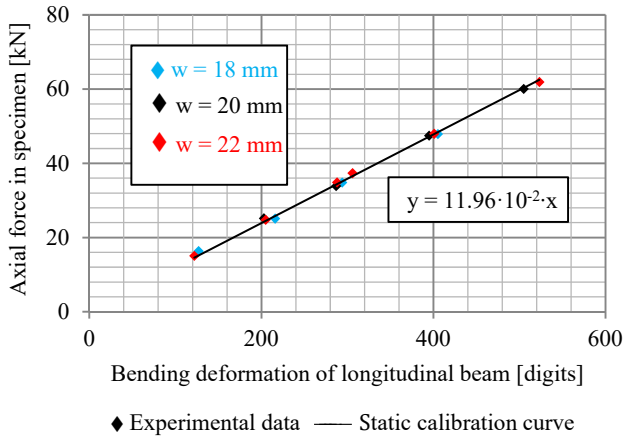

Fig. 10: Static calibration curve of ductile cast iron specimens (w = width of specimen)

Dynamic Calibration of the Test Device

Analogous to the static calibration, the dynamic calibration allows to read the preload from the accelerometer signal of the resonance-regulated test device. To determine the dynamic calibration factor, the calibration specimens are installed in the test device and operated on four different amplitudes. In each test the accelerometer measures the acceleration of the longitudinal bar. The control unit acquires the measured signal in digits via 12 bit AD converter. The dynamic calibration curve is given by the linear regression of the relationship between the force amplitude applied according to the calibration specimen and the acceleration signal of the frame elongation in digits.

The calibration results in Fig. 11 show that the change in stiffness of the specimen due to different width of 18 mm to 22 mm yields a different dynamic calibration factor respectively slope of the calibration curve. According to Fig. 12 the calibration factor changes furthermore with the level of pretension Three different levels were investigated.

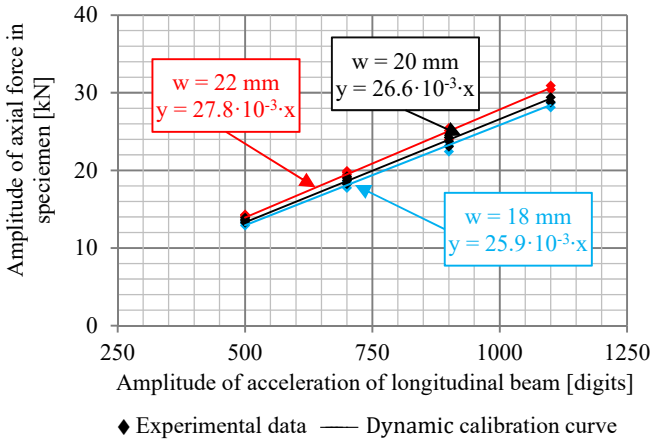

Fig. 11: Dynamic calibration curves of ductile cast iron specimens(w = width of specimen)

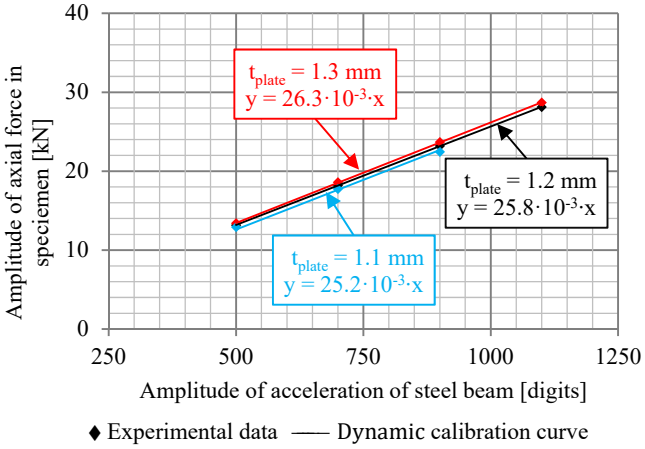

Fig. 12: Influence of the pretension (steel plate thickness) on the dynamic calibration curves of the ductile cast iron specimens with width = 18 mm (t_{plate} = thickness of pretension plate)

Both influences on the calibration factor that of stiffness and preload go along with a change in first natural frequency of the test device. Fig. 13 in fact demonstrates that the calibration factor can be simply defined as a function of the operating frequency. The calibration factors of all preloads, amplitudes and widths of cast iron specimen are plotted versus natural frequency. The linear regression curve was implemented in the control loop. Calibration factors are the slope (k_{d1}) and the offset (k_{d2}). For the tested specimens, the values k_{d1} and k_{d2} are $65.9 \cdot 10^{-3}$ and -10.22, respectively.

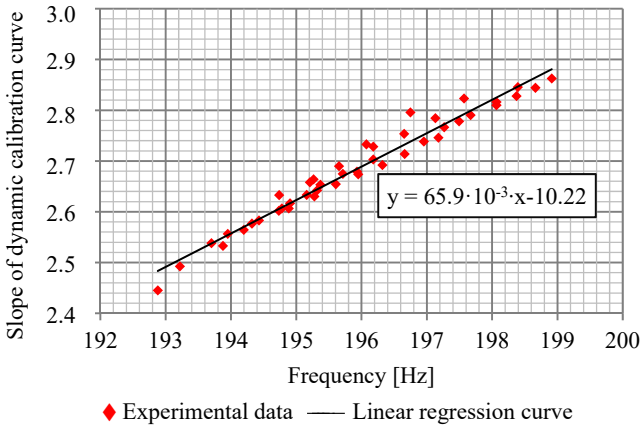

Fig. 13: Relationship between slope of dynamic calibration curve and oscillation frequency of ductile cast iron specimens

FATIGUE TESTS

To start the test, the control unit sweeps through a set of frequencies with which the AC magnets oscillates the resonance body. The resonance body is deflected in its first bending mode of vibration. Once the resonance frequency is detected by the control unit, it is fed back via a control loop (PI controller).

During the test run, the time-varying parameters of the resonance body are measured and recorded together with the corresponding number of load cycles. The time-varying parameters of the resonance include load amplitude, pretension force (mean stress), and test frequency. For the calibration samples, the time-variable parameters of the sample (pretension force and load amplitude) are also recorded. For selected specimens, the temperature at the nominal cross section of the specimen is additionally measured during the test.

As previously described, the specimens are statically preloaded with a pretension force and dynamically loaded with a constant load amplitude. The acceleration of the steel beam represents the controlled variable in order to keep the load amplitude constant during the test. Fig. 14 and Fig. 15 show the time-varying parameters of an exemplary test, plotted against the number of load cycles.

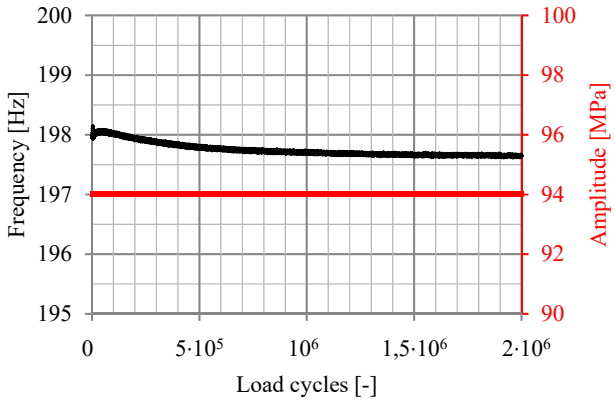

Fig. 14. Amplitude and oscillation frequency during the fatigue test with the amplitude of 94 MPa

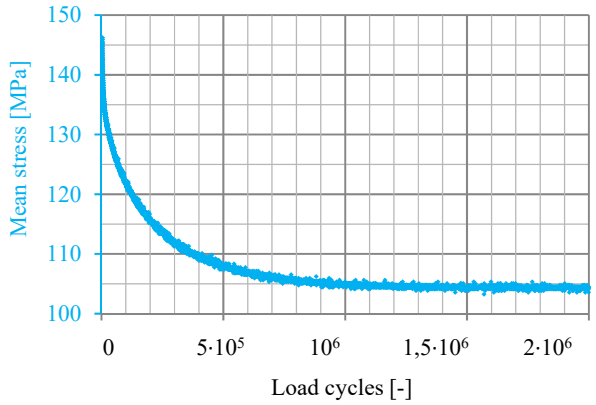

Fig. 15: Mean stress in the specimen during the fatigue test with the amplitude of 94 MPa

As can be seen in Fig. 14, the amplitude, which is regulated by the control unit, is constant during the test. The same is observed for the testing frequency (198 Hz), which decreases marginally. The mean stress of the specimen decreases until reaching a constant value after approximately 1.0 to 1.5 million load cycles (Fig. 15). As a readjustment of the pretension during the test is not possible, the observed loss of pretension is studied and quantified such that a prediction of pretension loss prior to the test is made possible. This predicted value of pretension loss should be than taken into account during the pre-stressing process such that the desired level of mean stress (and thus of stress ratio R) is reached at 1.5 million load cycles.

Loss of Pretension

The pretension losses occur in the initial phase of the test and can be categorized in three groups:

- Losses due to the hysteresis of the material,
- Losses due to the settling of the resonance frame,
- Losses due to the heating of the specimen during the test.

The first type of losses can be mitigated by pre-tensioning of the specimen at the level of the maximal stress expected during the test (sum of amplitude and pretension). After this first pre-loading, the specimen is released and pre-tensioned again at the desired level of pretension.

The other two types of losses cannot be eliminated. Because the readjustment of the pretension level is not possible, these losses have to be quantified and taken into account during the pretension procedure. Thus, the initial pretension to be applied on the specimen is the sum of the desired level of mean stress of the test and the expected pretension losses in the initial phase of the test.

Loss of pretension due to settling of the resonance body

As mentioned previously, the bolts of the crosspiece are loosened during the pre-stressing process, and the steel beams are pushed apart in order to set the steel plates. This means that the resonance frame is newly configured during each pretension process, and it sets during the first dynamic loading following.

The loss of pretension due to settling of the resonance frame is studied by comparing the loss within the first 100,000 load cycles of the first test performed after the pretension procedure with the loss of a subsequent test with the same pretension setup (Fig. 16). This procedure is repeated for different load amplitudes.

The results show that the loss caused by this settling varies between 15 MPa and 20 MPa and does not depend on the amplitude. The settling occurs within the first 60,000 load cycles after which the mean stress curves overlap. The further drop of pretension after 60,000, exhibited by both curves in Fig. 16, is caused by the losses due to the heating of the specimen.

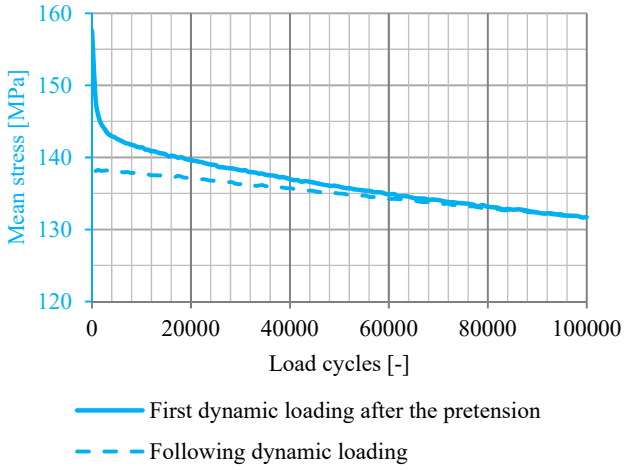

Fig. 16: Comparison of the tests with (first dynamic loading after the pretension) and without (the following dynamic loading) the losses of the pretension due to settling of the resonance body, tested with the amplitude of 100 MPa

Loss of pretension due to heating of the specimen

The specimen oscillates during the test with a frequency of approximately 200 Hz. The intrinsic dissipation and microscopic plasticity of the material at such a rate of oscillation cause the self-heating of the specimen (Favier et al, 2013; Torabian et al., 2016) and consequently the loss of pretension. Eventually a constant level of the temperature is reached, as an equilibrium of the heat created by the specimen and of the heat losses to the surrounding air is established. Fig. 17 shows an example of the loss of pretension due to heating of the specimen, tested with the amplitude of 94 MPa.

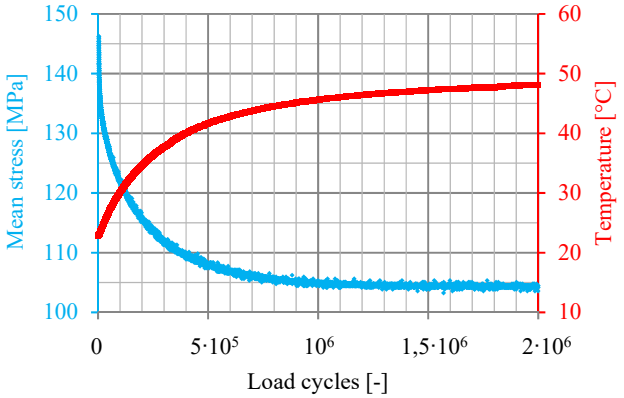

Fig. 17: Example of the loss of pretension due to heating of the specimen tested with the amplitude of 94 MPa

During the tests, the temperatures of nominal cross section of up to 50°C are measured. The temperature due to specimens self-heating is in relationship to the applied amplitude. The experimental results as well as

the power regression curve which describes the mentioned relationship, are given in Fig. 18.

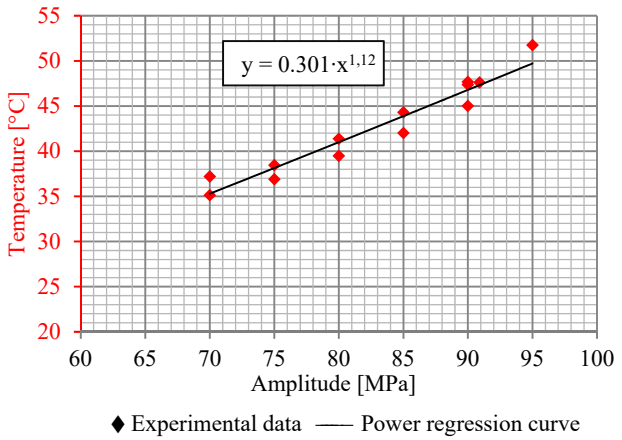

Fig. 18: Relationship between the applied amplitude and rise of temperature in the nominal cross-section of the specimen

The magnitude of decrease of the pretension caused by specimens self-heating depends on the applied load amplitude. Fig. 19 shows the relationship of the losses of pretension due to heating and the applied amplitude of the ductile cast iron specimens. The relationship follows a power curve. Losses of approximately 23 MPa are expected for an amplitude of 100 MPa.

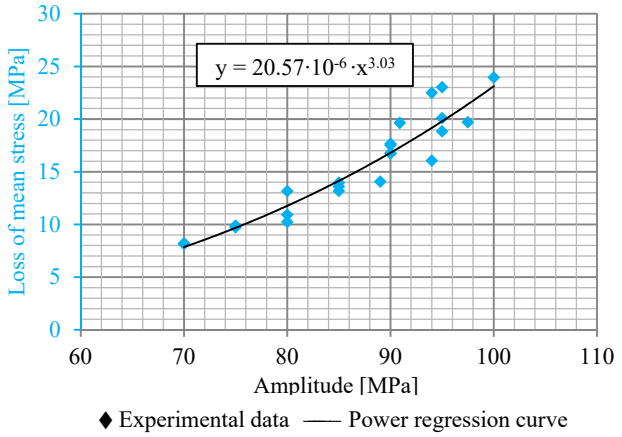

Fig. 19: Relationship between the applied amplitude and losses of pretension due to heating of the specimen

Different strategies to mitigate the loss of pretension due to heating of the specimen will be considered in future tests. One possibility is to implement an auxiliary cooling of the specimen in the system. The other possibility represents a preheating of the specimen at the level of the maximal temperature expected during the test (see Fig. 18).

Stop Criterion

Two termination criteria of the test are defined:

- Failure of the specimen: termination due to a drop in pretension force below a specified level of mean stress,
- Run-out termination if a specified number of load cycles is reached.

If the pretension force of the specimen drops significantly, a crack in the specimen can be assumed, and the test is terminated. The termination criterion for the preload force is a drop below a defined force level. The pretension level for the termination is usually set slightly above that of the load amplitude to prevent the situation in which the specimen is not continuously loaded and which would cause the system to go out of resonance.

If the initial mean stress is not sufficiently high, it may happen that the predefined level of pretension is reached due to pretension losses. For this reason, it is important to perform pre-tests and quantify the expected pretension losses as shown in previous section.

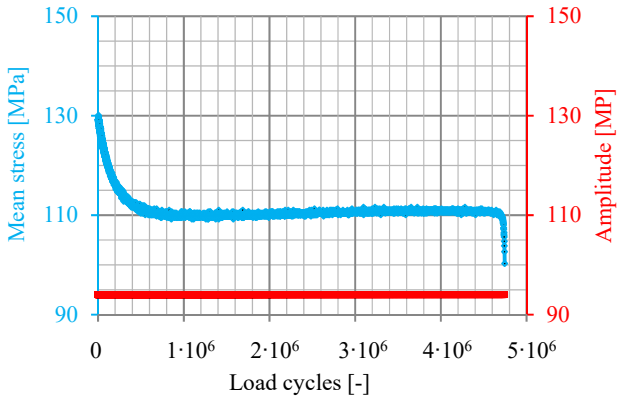

Fig. 20: Example of a test with specimen's failure with stop criterion set at 94 MPa

If the desired number of load cycles is reached with a constant preload force, the test is also completed. An example with stop criterion set at $2 \cdot 10^8$ load cycles is given in Fig. 21.

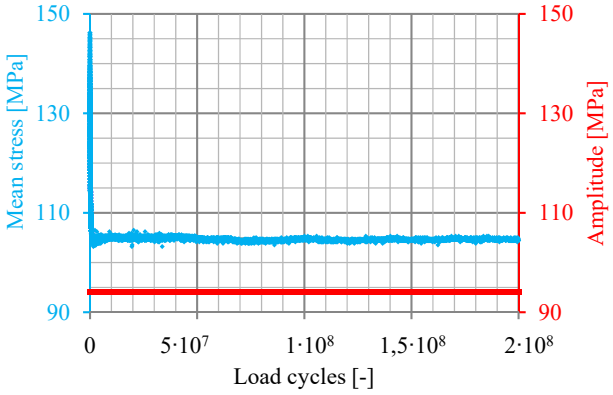

Fig. 21: Example of a run-out test with stop criterion set at $2 \cdot 10^8$ load cycles

CONCLUSIONS

The fatigue strength of the casted and welded structural components is of great importance for offshore wind turbines, which are subjected to a continuous cyclic loading. Experimental investigations on the fatigue strength serve to validate or expand the existing codes and regulations concerning the design of these components. In the range of very high cycle fatigue, which is defined for numbers of load cycles greater than

10^7, there are only few fatigue curves based on experiments. The main limiting factor for investigations in this range is the great duration required of such experiments.

In order to overcome these difficulties, a novel resonance-regulated test device with a test frequency of 200 Hz was developed. The operating principle of the device is based on the resonance at the level of the first natural frequency of the system composed of the testing device and the specimen. The oscillation at this frequency is induced in the system via electromagnets (Alt, 2007). The device is able to perform tests on axially loaded plate specimens with a thickness of up to 20 mm and a width of up to 40 mm. It allows testing with a maximum amplitude of 70 kN and a stress ratio of $0.1 \leq R \leq 0.5$.

The device generates pulsating tensile loads with constant amplitude. The mean stress in the specimen is achieved via its pretension prior to the test. At the beginning of the fatigue test, a pretension loss is observed. The loss is caused by the settling of the device, which is a consequence of the pretension procedure. Furthermore, the intrinsic dissipation and microscopic plasticity combined with high operating frequency cause self-heating of the specimen. The heated specimen expands, which causes a further loss of pretension. During the fatigue test the initially imposed level of pretension cannot be readjusted. Thus, the mentioned losses have to be taken into account when deciding on the level of pretension to be applied at the specimen prior to the test.

The resonance-based device represents a reliable testing technology for very high cycle fatigue test. As a resonance-regulated machine, the operating frequency is highly sensitive to changes in geometry or material properties of the specimen. The dynamic calibration factor is depending on the operating frequency. Another calibration may be required for a new type of specimen if the operating frequency changes. The calibration, pretension and testing procedures presented in this paper are based on the tests with ductile cast iron specimens (EN-GJS-18C-LT). These procedures can be repeated in the same manner for any other type of cast iron and steel specimens to be tested with the presented device.

As part of the research activities of the Institute for Steel Construction at Leibniz University Hannover, the fatigue strength curves for of ductile cast iron (EN-GJS-18C-LT) and butt welded joints are to be validated for the range of the very high cycle fatigue up to $2 \cdot 10^8$ load cycles using the presented test method. Additionally, tests on a conventional servo-hydraulic testing machine with testing frequency of 10 Hz will be performed. The comparison of the test results will allow for identification of any effect of testing frequency on the fatigue strength and on the fatigue crack initiation mechanism in the range below 10^7 load cycles.

ACKNOWLEDGEMENTS

The testing device was developed by Attila Alt. The development of the device as well as the presented studies have been carried out within the ForWind joint research project "ventus efficiens – Joint research for the efficiency of wind energy converters within the energy supply system", financially supported by the Ministry for Science and Culture in Lower Saxony, Germany as well as within the research project “HyConCast - Hybrid substructure of high strength concrete and ductile iron castings”, which is funded by the German Federal Ministry for Economic Affairs and Energy. The authors thank the Ministry for Science and Culture in Lower Saxony and the Federal Ministry for Economic Affairs and Energy for funding and all project partners for the cooperation.

REFERENCES

Alt, A (2007). *Prüfvorrichtung zur Dauerschwingprüfung von Prüflingen* (in English: *Testing device for very high cycle fatigue tests*), German patent DE 10204258 B4.

DNVGL-RP-C203 (2016). *Fatigue design of offshore steel structures,* DNV GL Recommended practice, DNV GL.

DNVGL-ST-0361 (2016). *Machinery for wind turbines,* DNV GL Standard, DNV GL.

DIN 18088-3 (2019). *Tragstrukturen für Windenergieanlagen und Plattformen – Teil 3: Stahlbauten* (in English: *Structures for wind turbines and platforms – Part 3: Steel structures*), DIN Deutsches Institut für Normung.

Favier, V, Phung, N-L, Ranc, N, Bretheau, T, Groslafaige, J, et al. (2013). “Microplasticity and energy dissipation in very high cycle fatigue,” Fatigue Design 2011, Senlis. https://hal.archives-ouvertes.fr/hal-00858854.

Furuya, Y (2010). "Size effects in gigacycle fatigue of high-strength steel under ultrasonic fatigue testing," *Procedia Engineering*, 2, 485-490.

ISO 1099 (2006). *Metallic materials – Fatigue testing – Axial force-controlled method*, International Organization for Standardization.

Seidel, M (2010). "Load characterization of axially loaded jacket piles supporting offshore wind turbines," *Proc Workshop “Gründung von Offshore-Windenergieanlagen”*, Karlsruhe.

Shirani, M, and Härkegård, G (2011). "Large scale axial fatigue testing of ductile iron for heavy section wind turbine components," *Engineering Failure Analysis,* 18(6), 1496-1510.

Schaumann, P, Alt, A, Kulikowski, J, Radulovic, L, and Steppeler, S (2017). “High-frequency resonance-regulated testing device for very high cycle axial fatigue testing of large-scale cast iron and steel specimens,” *Proc. of the Seventh International Conference on Very High Cycle Fatigue (VHCF7)*, Dresden, 323-329.

Schaumann, P, Keindorf, C, and Alt, A (2008). " Hochfrequente Ermüdungstests an Schweißverbindungen mit einem neu entwickelten Magnetresonanzprüfrahmen“ (in English: "High-frequency fatigue tests on welded joints with a newly developed resonance based testing device "), *Proc Symp "Große Schweißtechnische Tagung",* Dresden.

Schaumann, S, and Steppeler, S (2013). "Fatigue tests of axially loaded butt welds up to very high cycles," *Procedia Engineering*, 66, 88–97.

Stanzl-Tschegg, S (2014). "Very high cycle fatigue measuring techniques," *International Journal of Fatigue*, 60, 2-17.

Steppeler, S (2014). *Zum Ermüdungsverhalten von Stumpfnaht-verbindungen bei sehr hohen Lastwechselzahlen* (in English: *Very high cycle fatigue of butt welds*, PhD Thesis, Institute for Steel Construction, Leibniz University Hannover, Shaker Verlag.

Torabian, N, Favier, V, Ziaei-Rad, S, Adamski, F, Dirrenberger, J, and Ranc, N (2016). “Self-heating measurements for a dual-phase steel under ultrasonic fatigue loading for stress amplitudes below the conventional fatigue limit,” *Procedia Structural Integrity 2*, 1191-1198.

Zenner, H, and Buschermöhle, H (1996). *Vereinheitlichung von Proben für Schwingversuche* (in English: *Unification of specimens for fatigue tests*), FKM Vorhaben Nr. 198, issue 217.